

Single-channel analysis of an NMDA receptor possessing a mutation in the region of the glutamate binding site

Lesley C. Anson, Ralf Schoepfer, David Colquhoun and David J. A. Wyllie

*Department of Pharmacology and Wellcome Laboratory for Molecular Pharmacology,
University College London, Gower Street, London WC1E 6BT, UK*

(Received 29 February 2000; accepted after revision 23 May 2000)

1. Recombinant NR1a/NR2A(T671A) *N*-methyl-D-aspartate (NMDA) receptor-channels, which carry a point mutation in the putative glutamate binding site that reduces glutamate potency by around 1000-fold, have been expressed in *Xenopus laevis* oocytes and their single-channel properties examined using patch-clamp recording techniques.
2. Shut time distributions of channel activity were fitted with a mixture of five exponential components. The first three components in each distribution were considered to occur *within* a channel activation as they exhibited little or no dependence on agonist concentration.
3. Bursts of single-channel openings were defined by a critical gap length with a mean of 5.65 ± 0.37 ms. Shut intervals with a duration longer than this value were considered to occur *between* separate bursts of channel openings. Distributions of the lengths of bursts of openings were fitted with a mixture of four exponential components. The longest two components carried the majority of the charge transfer in the channel recordings and had means of 7.71 ± 1.1 and 37.7 ± 4.3 ms. The overall probability of a channel being open during a burst was high (mean 0.92 ± 0.01).
4. Brief concentration jumps (1 ms) of 10 mM glutamate were applied to outside-out patches so that a comparison between the macroscopic current relaxation and steady-state single-channel activity evoked by glutamate could be made. The decay of such macroscopic currents was fitted with a single exponential component with a mean of 32.0 ± 3.53 ms.
5. The good agreement between macroscopic current decay following brief agonist exposure and the value for the slowest component of the burst length distribution suggests that the bursts of openings that we identified in steady-state recordings represent individual activations of recombinant NR1a/NR2A(T671A) NMDA receptor-channels.
6. A new way of displaying geometric distributions is suggested, and the utility of a modified definition of the 'probability of being open within a burst' is discussed.
7. The single-channel data that we present in this paper support further the idea that the point mutation T671A in the NR2A NMDA receptor subunit affects mainly the ability of glutamate to remain bound to these channels.

The *N*-methyl-D-aspartate (NMDA) subtype of glutamate receptor-channel comprises NR1 and NR2 receptor subunits. The NR1 subunit is thought to contain residues that contribute to the binding site for the co-agonist, glycine (Kuryatov *et al.* 1994; Wafford *et al.* 1995; Hirai *et al.* 1996; Williams *et al.* 1996), whereas NR2 subunits contain the binding site for glutamate (Laube *et al.* 1997; Anson *et al.* 1998; Lummis *et al.* 1998). The point mutation which replaces a threonine residue at position 671 on the NR2A subunit with an alanine residue (henceforth referred to as NR2A(T671A)) results in a 1000-fold decrease in the potency of glutamate when these mutated subunits are co-expressed with NR1 subunits in *Xenopus* oocytes (Anson

et al. 1998). The nature of this change in potency is consistent with the idea that this mutation affects, primarily, the ability of glutamate to bind to the NMDA receptor, rather than affecting the ability of glutamate to open the channel once bound. To verify this, and to obtain further data concerning the effects of this mutation, we have carried out a systematic study of the single-channel kinetic properties of NR1a/NR2A(T671A) receptor-channels. Additionally we have performed concentration jump experiments to examine the properties of NR1a/NR2A(T671A) channel activations following brief exposure to glutamate.

A preliminary report of some of our findings has appeared (Anson *et al.* 1999).

METHODS

Oocyte preparation

Expression of recombinant NR1a/NR2A and NR1a/NR2A(T671A) NMDA receptor-channels in *Xenopus laevis* oocytes was similar to that described previously (see Béhé *et al.* 1995; Wyllie *et al.* 1996; Sivilotti *et al.* 1997). Briefly, *Xenopus* were killed by immersion in an overdose solution of 3-amino-benzoic acid ethyl ester (0.5%, pH to 6.8 with sodium bicarbonate). Death was confirmed by the subsequent destruction of the brain. Oocytes were removed, defolliculated and injected with cRNA encoding either NR1a and NR2A or NR1a and NR2A(T671A) subunits. Patch-clamp recordings were made after the removal of vitelline membranes between 3 and 10 days following injection.

Single-channel recordings

Steady-state single-channel activity of NR1a/NR2A(T671A) receptors was evoked by the application of 10–300 μM glutamate (in the presence of 20 μM glycine) to outside-out membrane patches. Such concentrations are about three orders of magnitude higher than those used for wild-type NR1a/NR2A NMDA receptor-channel steady-state recordings but were chosen as they gave a response comparable with that elicited by 100 nM glutamate (+ 20 μM glycine) in wild-type channels. Patches were held at -100 mV and bathed in an 'external' recording solution that contained (mM): 125 NaCl, 3 KCl, 1.25 $\text{Na}_2\text{H}_2\text{PO}_4$, 20 Hepes and 0.85 CaCl_2 (pH adjusted to 7.4 with NaOH). Patch pipettes were made from thick-walled borosilicate glass (Clark Electromedical, Reading, UK) and were filled with an 'internal' solution that contained (mM): 141 potassium gluconate, 2.5 NaCl, 10 Hepes and 11 EGTA (pH adjusted to 7.4 with KOH). These solutions were chosen to give a reversal potential of -100 mV for K^+ and Cl^- ions. Patch pipettes had resistances of 10–20 M Ω . Single-channel activity was recorded with an Axopatch-1D amplifier (Axon Instruments, Foster City, CA, USA) and recorded onto digital audiotape (Biologic DTR 1205, Biologic Instruments, Claix, France).

Concentration jump experiments

Fast concentration jumps on outside-out patches were performed as described previously (Wyllie *et al.* 1998). Briefly, two solutions flowing from either side of a piece of pulled theta glass were switched rapidly across an outside-out membrane patch. The control solution contained 20 μM glycine, while the test solution contained 10 mM glutamate in addition to 20 μM glycine. Patches were exposed to glutamate for either 1 ms or 100 ms and jumps were made every 5 s. The macroscopic agonist-evoked currents were filtered at 2 kHz and sampled at 10 kHz onto a computer hard disk via a CED 1401 Plus interface (CED Instruments, Cambridge, UK) using the computer program CJUMP. Individual jumps were averaged and the resulting mean current fitted (least squares) with exponential curves using the CJFIT program (available from <http://www.ucl.ac.uk/Pharmacology/dc.html>).

Analysis

Steady-state single-channel current data were replayed from DAT tape, filtered at 2 kHz and digitised at 20 kHz. The amplitudes of single-channel currents and their durations were measured using the SCAN program and analysed using the EKDIST program (Colquhoun & Sigworth, 1995; available from <http://www.ucl.ac.uk/Pharmacology/dc.html>). A resolution of 40 μs was imposed on both openings and closings in each data record, giving a false event rate of $< 10^{-6} \text{ s}^{-1}$. Distributions of shut times, burst lengths, total open time per burst and number of openings per burst were fitted with either mixtures of exponential or geometric components using the method of maximum likelihood. Bursts of

single-channel openings were defined by a critical gap length (t_{crit}) that was calculated to give equal numbers of mis-classified events, i.e. the number of gaps that were incorrectly assigned as being within a burst when they were in fact between bursts was equal to the number that were classified as being between when they were in fact within bursts (see Magleby & Pallotta, 1983; Clapham & Neher, 1984). Bursts of openings were aligned on their first opening and averaged for comparison with macroscopic concentration jump data (for details see Wyllie *et al.* 1998).

Logarithmic display of geometric distributions

Distributions such as that of the number of open periods per burst are expected to be described by mixtures of geometric distributions (Colquhoun & Hawkes, 1982). Observations are best fitted by maximum likelihood, as described by Colquhoun & Sigworth, (1995). The conventional display of these distributions makes it hard to see, and compare, the tail of the distribution, which often has low amplitude. In the case of distributions of durations (e.g. shut times), this problem is usually solved by showing the results as distributions of log(duration), the square root of the number values normally being plotted, as here (Blatz & Magelby, 1986; Sigworth & Sine, 1987). This is not feasible in the case of a discrete variable such as the number of open periods per burst. This number, r say, can take only integer values, $r = 1, 2, 3, \dots$, these integer values cannot be grouped into bins whose boundaries are equally spaced on a logarithmic scale. We have therefore introduced a display for geometric distributions which is analogous to that for log(duration).

If the number of times a value equal to r is observed is denoted $f_r(r)$, then the display is constructed by plotting

$$\sqrt{(rf_r(r))} \text{ against } \log(r). \quad (1)$$

Recalling that the probability density function, $g(x)$ say, of $x = \log(t)$ is given by

$$g(x) = tf(t) \quad (2)$$

(Colquhoun & Sigworth, 1995), the new plot is seen to bear a close analogy to the distribution of log(duration), and becomes identical with the latter for geometric distributions with large means (it is close when the mean value of r is greater than 10 or so). In the case of durations, the observations are grouped into bins whose boundaries are equally spaced on a logarithmic scale, and the frequency of observations in the lowest bins is low because the lowest bins are narrow. In the case of an integer variable the bin width cannot be altered, but the same effect is obtained by multiplying the observed frequency by r (compare (1) and (2)).

The simple geometric distribution with mean μ is

$$P(r) = \frac{1}{\mu} \left(1 - \frac{1}{\mu}\right)^{r-1}. \quad (3)$$

Since r is a discrete variable, these probabilities exist only at $r = 1, 2, 3, \dots$. If we define $G(r) = rP(r)$, then the ratio of two successive terms is

$$\frac{G(r)}{G(r-1)} = \frac{1 - \frac{1}{\mu}}{1 - \frac{1}{r}}, \quad (4)$$

which is greater than 1 if and only if $r < \mu$. Thus $G(r) = rP(r)$ rises to a maximum at a value that is the integer part of μ (the mean rounded down to the nearest integer), and then declines. If μ happens to be an integer, which in general will not be so, then there will be two equal maxima, at $r = \mu - 1$ and at $r = \mu$. The envelope of the display, found by treating r as a continuous variable, has a

maximum at $r = -1/\ln(1 - 1/\mu)$, which approaches $\mu - 0.5$ for large values of μ . Thus the peak of the display is close to the mean of the distribution, like the analogous distribution of $\log(\text{duration})$, for which the peak is at the mean, τ .

For geometric distributions with means smaller than 10 or so, the new plot has a different shape from the distribution of $\log(\text{durations})$ and this is illustrated in Fig. 1. The probabilities exist, of course, only at $r = 1, 2, 3, \dots$, and so should be plotted as points or vertical lines at these values of r . Joining these points with straight lines, as in Fig. 1*B* and *C*, has no statistical meaning, but is a purely cosmetic device that is intended to increase legibility. Figure 1*A* shows the conventional histogram display of the simple geometric distribution, $P(r)$, with means $\mu = 1.1, 2, 5$ and 10 , while Fig. 1*B* shows the same distribution displayed as points rather than bins. Figure 1*C* shows the same distributions, but plotted in the new way, as $\sqrt{rP(r)}$ against $\log(r)$. This display emphasises large r values, and, because there will be few observations at the largest r values, it will be sensible to pool the observed values for a range of r values at the right-hand end of the plot. This procedure is illustrated in Fig. 5, in which observed frequencies, $f_r(r)$ (not the

values of $r f_r(r)$), are averaged in groups of 5 for $r > 22-26$. All results are given as means \pm standard deviation of the mean (s.d.m.)

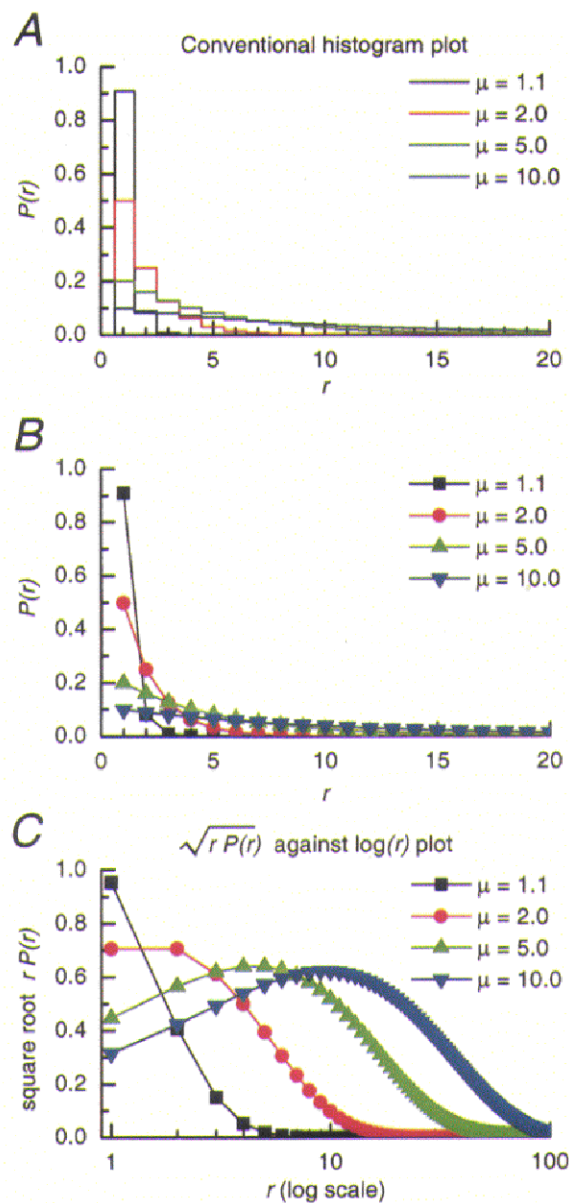
RESULTS

Single-channel conductance

Figure 2*A* shows a selection of NR1a/NR2A(T671A) single-channel currents recorded at a variety of holding potentials between -100 and -20 mV. Transitions between a main and a sub-conductance level are clearly visible in some of the records. The current-voltage plots for these two conductance levels are shown in Fig. 2*B* and give a mean slope conductance for the main level of 50 ± 2 pS and for the sub-conductance level of 40 ± 3 pS ($n = 5$). These values are indistinguishable from the conductances reported for wild-type NR1a/NR2A NMDA receptor-channels and many 'high conductance'-type NMDA receptor-channels found in neurones in the central nervous system when

Figure 1. Illustration of a new type of display for geometric distributions

A, the conventional histogram display of four simple geometric distributions, with means of 1.1, 2.0, 5.0 and 10.0. *B*, the same distributions as depicted in *A*, but displayed as points rather than bins. *C*, a new type of display for data that are distributed geometrically. The value of r is plotted on a logarithmic scale on the abscissa and the square root of the product of r and the frequency with which r occurs is plotted on the ordinate. This results in a plot that has a peak of close to the mean of the distribution, as described in Methods.



recorded using comparable solutions (for a review see Cull-Candy *et al.* 1995). The stability of channel activity in data records was examined for all patches and an example of such a record is illustrated in Fig. 2*C*. Channel activity in this patch was evoked by 100 μM glutamate (+ 20 μM glycine) and the patch was held at -100 mV. As has been documented previously for NMDA receptor-channels, the mean open period of channel openings exhibited very little variation for the duration of the patch recording. The variability in the overall open probability (P_{open}) of the data record stemmed largely from the variability in the (means of 100) shut time values (for other examples see Stern *et al.* 1992; Wyllie *et al.* 1996).

Shut time distributions

Figure 3 shows three shut time distributions for NR1a/NR2A(T671A) NMDA receptor-channels from the same patch but recorded during the application of either 10, 30 or 100 μM glutamate (+ 20 μM glycine). The applications

were made in the order 100, 30 then 10 μM glutamate with returns to 'control' solution between each agonist application. Each shut time distribution was well described by a mixture of five exponential components. This figure shows that the major effect of increasing the agonist concentration is to reduce the value of the time constant of both the fourth and fifth components. Increasing the agonist concentration had little effect on the value of the time constant of the first three components (or their relative areas). The dashed line superimposed on the distributions shown in Fig. 3*B* and *C* is the fit obtained from the distribution illustrated in Fig. 3*A*, scaled to take account of the different number of events in each distribution. Such a result would be expected if shut times contained within the last two components occurred between separate activations of NR1a/NR2A(T671A) NMDA receptor-channels and those found in the first three components occurred within an individual activation. Values for the overall P_{open} of each data stretch were clearly dependent on the agonist concentration and were 0.0016

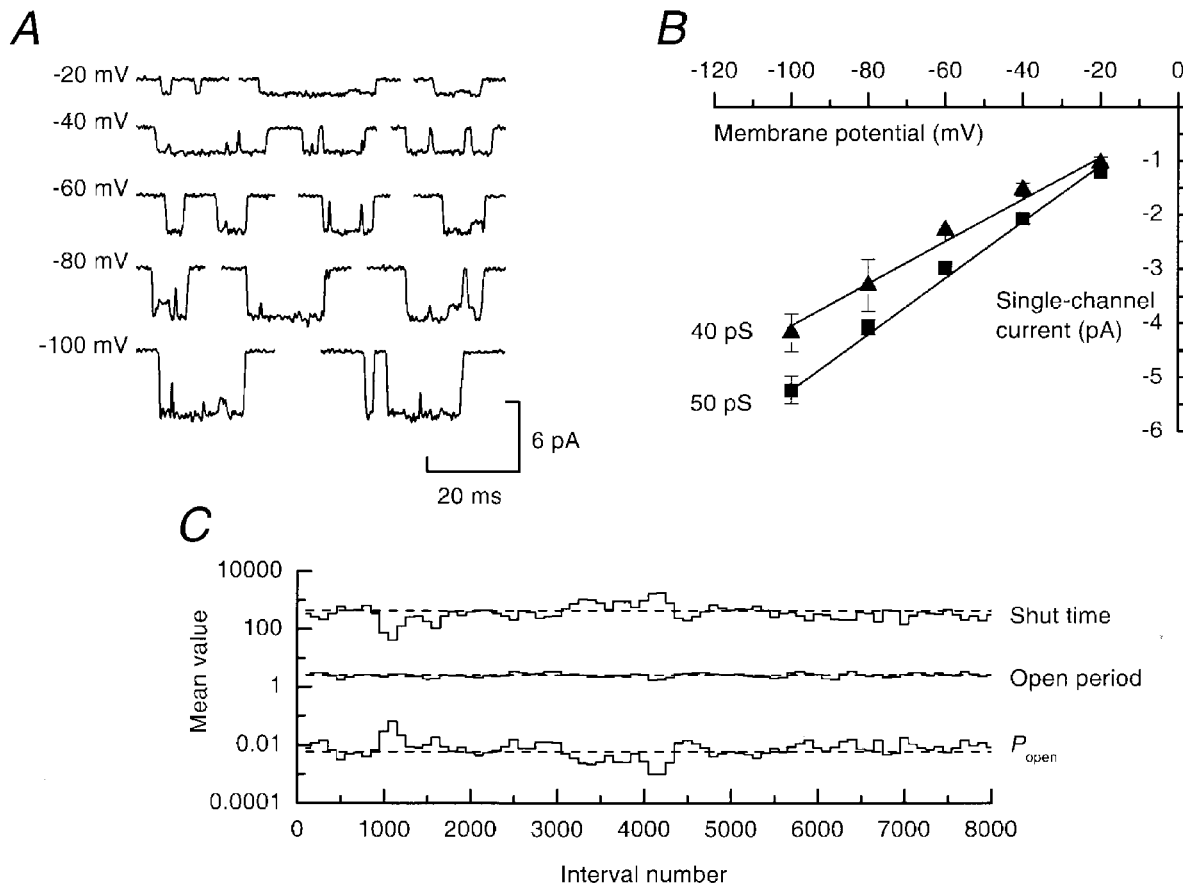


Figure 2. Single-channel current–voltage relationships and kinetic parameter stability plots for NR1a/NR2A(T671A) NMDA receptor-channels

A, examples of single-channel currents recorded at a series of holding potentials from -100 mV to -20 mV. The presence of a sub-conductance level is clearly visible. *B*, single-channel current–voltage plot for the two conductance levels. Data points are the mean (\pm s.d.m.) of the fitted amplitudes of single-channel currents recorded from five experiments. The lines show the least-squares fit of the data and give slope conductances of 50 ± 2 and 40 ± 3 pS for main and sub-conductance levels, respectively. *C*, stability plot for an experiment where channels were activated by 100 μM glutamate (in the presence of 20 μM glycine) at a holding potential of -100 mV. An average of 100 values (in increments of 50 values) was calculated for each of the parameters shown. The overall mean value for each parameter is indicated by the dashed lines.

Table 1. Kinetic parameters for NR1a/NR2A(T671A) single-channel currents

		τ_1 (μ s)	τ_2 (ms)	τ_3 (ms)	τ_4 (ms)	τ_5 (ms)	Distribution mean (ms)
All recordings ($n = 15$)	Shut time	21 ± 1 ($60 \pm 2\%$)	0.190 ± 0.010 ($14 \pm 1\%$)	1.28 ± 0.04 ($10 \pm 1\%$)	433 ± 145 ($6 \pm 1\%$)	3164 ± 686 ($10 \pm 1\%$)	375 ± 86
	Burst length	48 ± 3 ($44 \pm 3\%$)	0.484 ± 0.069 ($11 \pm 2\%$)	7.71 ± 1.10 ($26 \pm 2\%$)	37.7 ± 4.3 ($19 \pm 2\%$)	—	9.42 ± 1.39
	Open time per burst	49 ± 4 ($43 \pm 3\%$)	0.418 ± 0.051 ($11 \pm 2\%$)	7.26 ± 1.03 ($26 \pm 2\%$)	34.8 ± 3.7 ($20 \pm 2\%$)	—	8.71 ± 1.27
	Burst $P_{\text{open}} = 0.92 \pm 0.01$						
10 μ M glutamate ($n = 4$)	Shut time	20 ± 1 ($57 \pm 2\%$)	0.197 ± 0.022 ($12 \pm 1\%$)	1.25 ± 0.07 ($9 \pm 1\%$)	739 ± 330 ($10 \pm 1\%$)	5317 ± 1764 ($12 \pm 2\%$)	656 ± 183
	Burst length	44 ± 3 ($52 \pm 4\%$)	0.529 ± 0.127 ($12 \pm 5\%$)	6.22 ± 0.36 ($26 \pm 4\%$)	35.1 ± 3.3 ($10 \pm 2\%$)	—	5.50 ± 1.20
	Open time per burst	45 ± 4 ($51 \pm 4\%$)	0.451 ± 0.119 ($13 \pm 5\%$)	5.89 ± 0.45 ($26 \pm 4\%$)	32.6 ± 3.5 ($10 \pm 2\%$)	—	5.12 ± 1.17
	Burst $P_{\text{open}} = 0.92 \pm 0.02$						
100 μ M glutamate ($n = 6$)	Shut time	22 ± 2 ($58 \pm 5\%$)	0.185 ± 0.019 ($15 \pm 2\%$)	1.30 ± 0.04 ($10 \pm 1\%$)	154 ± 23 ($5 \pm 1\%$)	1948 ± 448 ($12 \pm 3\%$)	284 ± 110
	Burst length	43 ± 1 ($44 \pm 5\%$)	0.364 ± 0.066 ($8 \pm 2\%$)	6.26 ± 1.40 ($25 \pm 5\%$)	28.5 ± 4.4 ($23 \pm 4\%$)	—	7.86 ± 1.42
	Open time per burst	43 ± 5 ($43 \pm 5\%$)	0.350 ± 0.069 ($9 \pm 2\%$)	6.05 ± 1.40 ($25 \pm 5\%$)	26.9 ± 4.2 ($23 \pm 4\%$)	—	7.38 ± 1.39
	Burst $P_{\text{open}} = 0.93 \pm 0.01$						

Time constants for each component (τ_1 to τ_5) are given \pm s.d.m., together with their percentage areas (in parentheses).

(10 μ M glutamate), 0.0091 (30 μ M) and 0.029 (100 μ M). The mean values for all shut times are given in Table 1. Additionally Table 1 documents the values for shut time components recorded in patches where the agonist concentration was either 10 or 100 μ M.

Properties of bursts of NR1a/NR2A(T671A) NMDA receptor-channel openings

The fact that the first three components in each shut time distribution obtained in this series of experiments were independent of the agonist concentration used to elicit the single-channel activity allowed us to separate bursts of channel openings based on a t_{crit} that was calculated between the third and fourth components in each shut time distribution. Overall the mean t_{crit} was 5.65 ± 0.37 ms ($n = 15$ recordings from 11 patches); for patches exposed to 10 μ M glutamate the mean t_{crit} was 5.42 ± 0.60 ms ($n = 4$), while for patches where the glutamate concentration was 100 μ M it was 5.12 ± 0.32 ms ($n = 6$). Distributions of burst lengths were fitted consistently with a mixture of four exponential components and an example of such a distribution is shown in Fig. 4A. The mean values for each of these components are listed in Table 1. The dashed line superimposed on this distribution is the distribution of activation lengths of wild-type NR1a/NR2A NMDA receptor-channels taken from data published in Wyllie *et al.* (1998) and has an overall mean of 35.8 ms. This illustrates

the fact that, on average, the longest activation lengths of NR1a/NR2A(T671A) NMDA receptor-channels are around an order of magnitude shorter than the longest activations seen with wild-type NR1a/NR2A NMDA receptor-channels. It should be pointed out that for our comparison between NR1a/NR2A(T671A) and wild-type NR1a/NR2A NMDA receptor-channels we wish to compare individual activations of a single NMDA receptor complex (for a rigorous definition of what we mean by an *individual activation* of a channel the reader is referred to the Discussion in Wyllie *et al.* 1998). Our estimate of what constitutes an activation is referred to here as a burst of openings, whereas the equivalent grouping of openings for wild-type receptor-channels was referred to as a super-cluster by Wyllie *et al.* (1998).

Figure 4B shows 'average' bursts taken from each of the four components in the burst length distribution, while Fig. 4C illustrates the average current produced from aligning (on their first opening) all bursts in the data record. This current is fitted with a sum of four exponentials with the time constants *fixed* to the values obtained from the burst length distribution (see Wyllie *et al.* 1998 for details and the theory behind this procedure). This procedure emphasises the fact that more than 98% of the charge transfer recorded in this patch was carried by channel activations that reside in the third and fourth components of the burst length distribution.

Distributions of total open time per burst were also examined to allow us to determine the P_{open} during a burst. Such distributions were fitted with a mixture of four exponential components (mean values are given in Table 1). This type of distribution for the experiment illustrated in Fig. 4 is shown as Fig. 5A. Again, for comparison with wild-type NR1a/NR2A NMDA receptor-channels, the dashed line superimposed on this distribution is the average fit of histograms of total open time per super-cluster taken from data reported in Wyllie *et al.* (1998). The overall mean P_{open} within a burst for NR1a/NR2A(T671A) NMDA receptor-channels was 0.92 ± 0.01 , whereas for wild-type NR1a/NR2A NMDA receptor-channels the mean P_{open} within an individual activation is 0.35 ± 0.05 (see Table 1, Wyllie *et al.* 1998).

Since NR1a/NR2A(T671A) NMDA receptor-channel burst lengths are shorter in duration than wild-type activations we would expect there to be fewer open periods per burst of NR1a/NR2A(T671A) channel activity. This indeed was confirmed. Figure 5B shows the distribution of number of open periods per burst for the experiment illustrated in Figs 4 and 5A. This distribution is fitted with a mixture of three geometric components and is shown in the new display format we described in the Methods. Figure 5C and D shows distributions of number of open periods per burst obtained by pooling data obtained from individual experiments. For NR1a/NR2A(T671A) NMDA receptor-channel activations (Fig. 5C) this distribution gave means (and areas) of 1.14 ± 0.02 ($45 \pm 3\%$), 3.34 ± 0.38 ($43 \pm 2\%$) and 10.7 ± 1.5 ($12 \pm 5\%$), while for wild-type NR1a/NR2A receptor

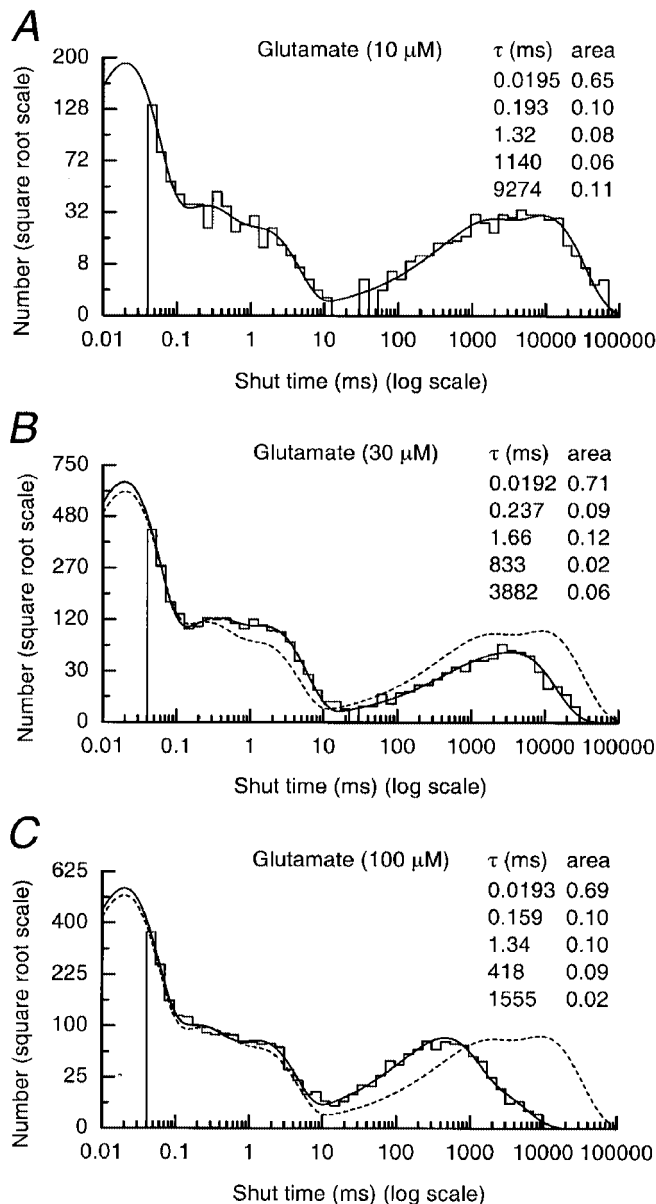


Figure 3. Shut time distributions for NR1a/NR2A(T671A) NMDA receptor-channels activated by different concentrations of glutamate

A, shut time distribution for NR1a/NR2A(T671A) NMDA receptor-channels activated by 10 μM glutamate (+ 20 μM glycine). The distribution is fitted with a mixture of five exponential components with means (and areas) as indicated. The fit predicts 2657 events and 1089 were included in the distribution which has a mean of 1069 ms. **B** and **C**, shut time distributions for the same patch as data in **A**, but in which the channels were activated by either 30 μM (**B**) or 100 μM (**C**) glutamate. Again each distribution is fitted with a mixture of five exponential components with means (and areas) as indicated; 2982 events were included in the distribution shown in **B** and 8374 events are predicted by the fit. The overall mean of this distribution is 250 ms. For **C**, the fit predicts 7133 events, while 2656 were included and the overall mean of this distribution is 69 ms. The dashed lines in **B** and **C** indicate the fit obtained from the data shown in **A**, scaled to take account of the different number of events in each distribution. Note that the time constants (and their respective areas) for the first three components in each distribution are similar.

activations (Fig. 5D) the mean values (and areas) for the geometric components were 1.33 ± 0.04 ($60 \pm 7\%$) 5.27 ± 0.97 ($25 \pm 6\%$) and 31.5 ± 5.3 ($15 \pm 4\%$). The overall mean number of open periods per burst for NR1a/NR2A(T671A) NMDA receptor-channels was 3.19 ± 0.25 . This value is less than the mean number of open periods per super-cluster for wild-type NR1a/NR2A NMDA receptor-channels (6.84 ± 1.11), as is obvious from comparison of Fig. 5C and D, and from a randomisation test ($P = 0.00014$).

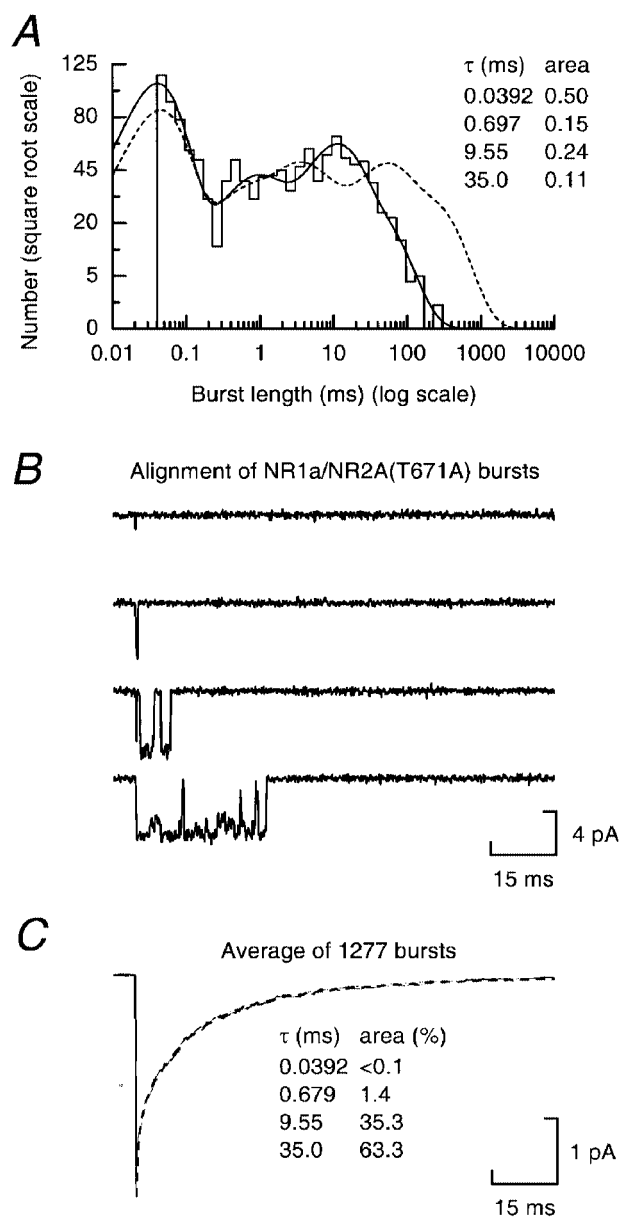
Concentration jump experiments

As an alternative approach to estimate the duration of individual activations of recombinant NR1a/NR2A(T671A) NMDA receptor-channels, we performed rapid concentration jumps on excised membrane patches and recorded the resulting macroscopic current activity. Examples of two individual jumps are shown in Fig. 6A. Openings (and closings) of individual ion channels can be seen clearly in

each of these sweeps. The trace shown as an inset to the upper panel is the liquid junction potential recorded at the end of this particular experiment. The average of ninety such concentration jumps is shown in Fig. 6B and the decay of this macroscopic current, after the agonist concentration was reduced to zero at the end of the pulse, was adequately described by a single exponential with a time constant of 28 ms. On average the mean decay time constant of currents evoked by the application of 10 mM glutamate for 1 ms was 32.0 ± 3.53 ms ($n = 5$). For comparison, an example of a macroscopic current recorded from a patch containing wild-type NR1a/NR2A NMDA receptor-channels is superimposed on the NR1a/NR2A(T671A) current trace and scaled to give an equivalent peak response (trace originally published as Fig. 6B in Wyllie *et al.* 1998). Two exponential components are required to fit adequately the decay of such currents and we have reported previously that

Figure 4. Burst length distribution and alignment of bursts for NR1a/NR2A(T671A) NMDA receptor-channels

A, distribution of NR1a/NR2A(T671A) NMDA receptor-channel burst lengths from an experiment in which channels were activated by 100 μ M glutamate (+ 20 μ M glycine). The distribution is fitted with a mixture of four exponential components with means and areas as indicated (continuous line). The distribution contains 1286 bursts and the fit predicts 1929 events. The overall mean of this distribution is 6.08 ms. The dashed line is the fit of wild-type NR1a/NR2A activation lengths, and is taken from data published in Wyllie *et al.* (1998) (Fig. 3A). The fit is scaled to take account of the different number of events contained in each distribution and has an overall mean of 35.8 ms. The values of the time constants (and their areas) for the wild-type NR1a/NR2A distribution are 42 μ s (39%), 0.38 ms (8%), 1.88 ms (8%), 4.08 ms (14%), 40.6 ms (17%) and 201 ms (14%). *B*, examples of four NR1a/NR2A(T671A) bursts taken from the same experiments as illustrated in *A*. These events are an attempt to represent the 'average' burst in each of the four components of the distribution. The upper trace in panel *B* has a duration of around 40 μ s and as such does not reach its full amplitude due to the fact that the data have been filtered at 2 kHz. *C*, current trace obtained from the alignment and averaging of the 1286 bursts recorded in this experiment. The decay of this current is fitted with a sum of four exponential components (dashed line) with the time constants fixed to the values from the burst length distribution illustrated in *A*.



the mean values for these two time constants are 70.8 ± 11.9 ms (relative amplitude $59 \pm 8\%$) and 350.1 ± 39.4 ms ($41 \pm 8\%$) (Wyllie *et al.* 1998).

In addition to brief concentration jumps we also carried out jumps in which patches were exposed to agonist for longer periods of time. As we propose that the point mutation NR2A(T671A) affects the ability of glutamate to bind to the

NMDA receptor-channel (most probably by affecting a dissociation rate constant; see Discussion) we used these longer jumps to ensure that we evoked currents whose maximum amplitude reflected the 'peak' response for the agonist concentration used (i.e. that the duration of the application did not prevent the current from reaching a plateau response). Figure 7A shows two individual sweeps

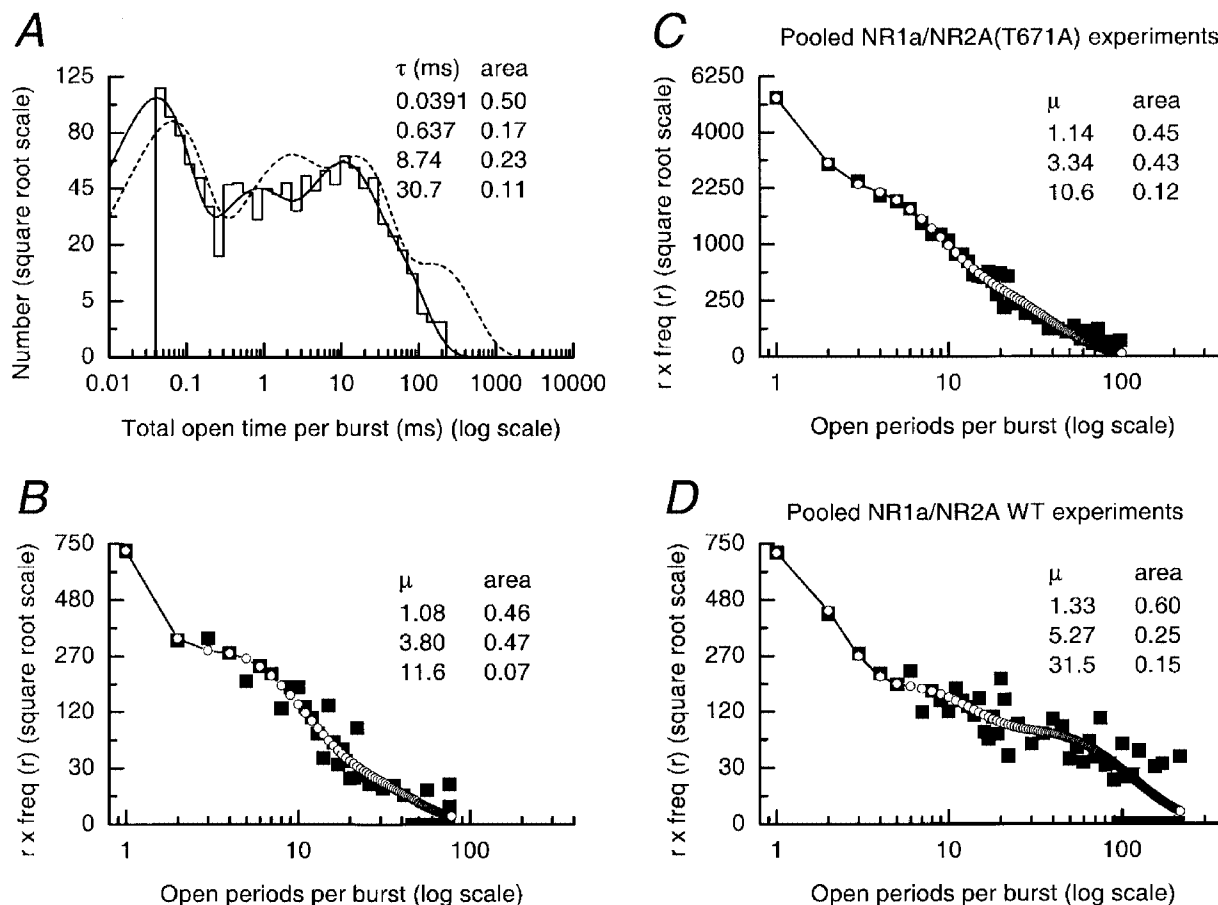


Figure 5. Distributions of total open time per burst and number of open periods per burst for NR1a/NR2A(T671A) and wild-type NR1a/NR2A NMDA receptor-channels

A, distribution of total open time per burst (for data illustrated in Fig. 4A) fitted with a mixture of four exponential components. The fit predicts 1917 events while the distribution contains 1286. The overall mean of this distribution is 5.41 ms. The dashed line is the fit of the equivalent distribution for wild-type NR1a/NR2A bursts and has an overall mean of 12.5 ms (data from Wyllie *et al.* 1998). The values of the time constants (and their areas) for the wild-type NR1a/NR2A distribution are 63 μ s (41%), 1.60 ms (22%), 14.7 ms (30%) and 150 ms (7%). *B*, distribution of number of open periods per burst for a typical recording of NR1a/NR2A(T671A) receptor-channel activity (same experiment as in *A*), and plotted in the new way, as $\sqrt{(rf_r(r))}$ against $\log(r)$, where $f_r(r)$ is the observed frequency of bursts that appear to contain r open periods (see Methods). These observed values are shown as filled squares, and the corresponding fitted values are shown as open circles (these have been joined by straight lines for the sake of legibility). The observed frequencies have been averaged in groups of 5 above $r = 26$. This distribution is fitted with a mixture of three geometric components and has an overall mean of 3.10. *C*, distribution of number of open periods per burst obtained by pooling data from NR1a/NR2A(T671A) NMDA receptor-channel recordings. Again this distribution is fitted with a mixture of three geometric components with means and areas as indicated and has an overall mean of 3.19. The observed frequencies have been averaged in groups of 5 above $r = 25$. *D*, distribution of number of open periods per burst obtained by pooling data from wild-type NR1a/NR2A NMDA receptor-channel recordings fitted with a mixture of three geometric components. The overall mean of this distribution is 6.84. The observed frequencies have been averaged in groups of 5 above $r = 22$.

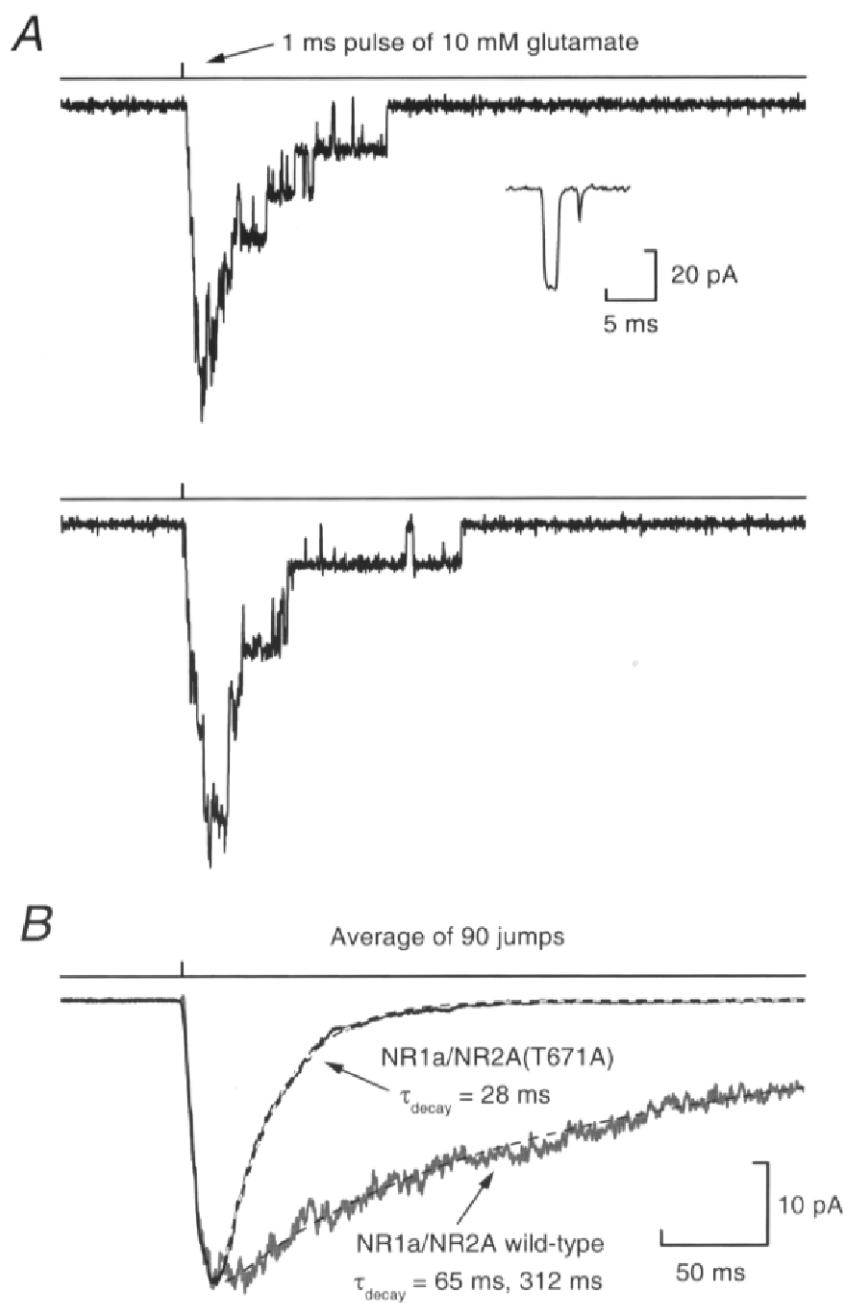


Figure 6. NR1a/NR2A(T671A) NMDA receptor-channel currents elicited by brief concentration jumps

A, two examples of individual sweeps recorded in an outside-out patch following a 1 ms application of 10 mM glutamate. Single-channel events of around 5 pA in amplitude are clearly visible in each of the current traces. The inset in the upper figure shows the liquid junction potential recorded at the end of the experiment when the membrane patch was ruptured by applying positive pressure. The difference in the ionic strengths between the glycine-containing 'control' solution and the glutamate + glycine 'test' solution was sufficient to allow the detection of a junction potential. The calibration bar refers to the junction potential current trace only. B, the average of ninety such jumps as illustrated in A. The decay of this current is described by a single exponential component with a time constant of 28 ms. Superimposed on this average is an example of a recording made from wild-type NR1a/NR2A recombinant NMDA receptor-channels to illustrate the difference between the deactivation rates of the two receptor combinations. The wild-type recording is taken from data from Wyllie *et al.* (1998) and has been scaled to give a similar 'peak' to that of the average for the NR1a/NR2A(T671A) trace and as such only the time base indicated on the calibration bar applies to the wild-type recording. Calibration bars in B also apply to NR1a/NR2A(T671A) channel recordings shown in A.

recorded from an outside-out patch exposed to 10 mM glutamate for 100 ms. The mean of thirty jumps is shown in Fig. 7*B*. On average the decay at the end of the '100 ms' jumps could be fitted with a single exponential component with a time constant of 31.0 ± 3.36 ms ($n = 13$). However, the decay of the current illustrated in Fig. 7*B* has been fitted with a sum of two exponential components whose time constants have been *fixed* to the values we obtained for the mean lengths of NR1a/NR2A(T671A) NMDA receptor-channel bursts found in the last two components of the burst length distribution. In other words the time constants from the burst length distributions and the decays of the macroscopic currents elicited by a concentration jump are in good agreement. This is to be entirely expected of a Markov process (for a precise description of the conditions for which this is to be expected see the Appendix of Wyllie *et al.* 1998). Again for comparison with wild-type NR1a/NR2A NMDA receptor-channels an example of a current evoked by a 100 ms application of 1 mM glutamate has been superimposed on the NR1a/NR2A(T671A) trace (Fig. 7*C*).

DISCUSSION

This paper describes the single-channel activity of an NMDA receptor-channel carrying a point mutation that reduces glutamate potency by around 1000-fold (Anson *et al.* 1998). The nature of the single-channel activations observed in our patch-clamp recordings is entirely consistent with the notion that the mutation of the threonine residue at position 671 on the NR2A subunit to an alanine residue affects, primarily, the ability of glutamate to remain bound to this receptor.

Nature of NR1a/NR2A(T671A) bursts

The single-channel conductance of NR1a/NR2A(T671A) activations were indistinguishable from those of wild-type receptors, indicating that this mutation has no effect on the ion permeation characteristics of NMDA receptor-channels. This of course is not surprising given the fact that this threonine residue is located in the S2 domain of the NR2 subunit well away from residues that are thought to influence the properties of the ion channel pore. In order to isolate individual activations of NR1a/NR2A(T671A) NMDA receptor-channels we analysed shut time distributions

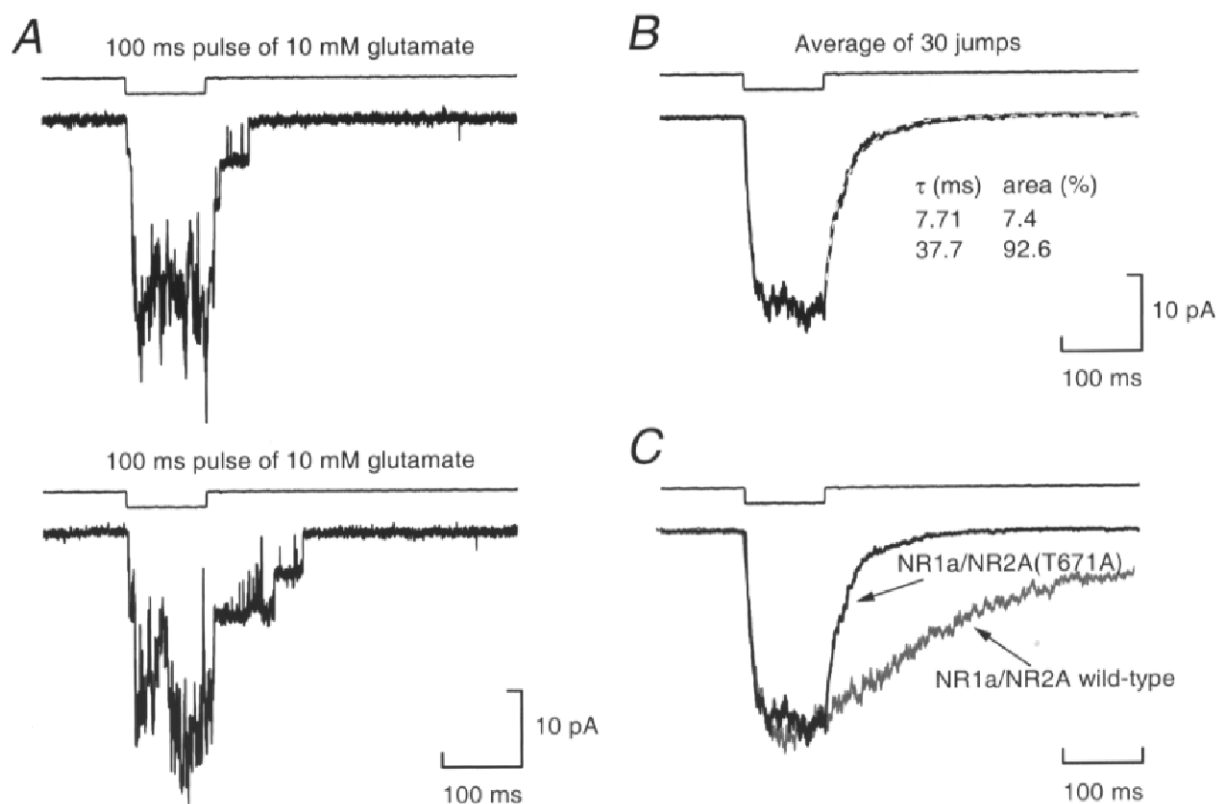


Figure 7. NR1a/NR2A(T671A) NMDA receptor-channel currents elicited by 100 ms applications of glutamate: comparison of the deactivation rates with burst lengths

A, examples of two individual sweeps recorded in response to the application of 10 mM glutamate for 100 ms. In this figure the trace above each of the recordings is the junction potential recorded at the end of the experiment following the rupturing of the membrane patch. *B*, the average of thirty such jumps is shown with the decay of this current fitted with a sum of two exponential components with the time constants *fixed* to the values obtained from analysis of NR1a/NR2A(T671A) single-channel burst lengths. *C*, comparison of NR1a/NR2A(T671A) and wild-type NR1a/NR2A responses evoked by 100 ms application of 10 mM glutamate (in the case of mutated receptors) or 1 mM glutamate (in the case of wild-type receptors).

to be the case, so no qualitative distinction between the two hypotheses can be made on the basis of these observations. However, we have also observed that the probability that the channel is open during an activation is much higher for mutant receptors (0.92) than for wild-type receptors (0.35). This 'burst P_{open} ' rises towards 1 as β is increased in Scheme 1. However, it goes through a minimum and also approaches 1 for very small β , because in this case openings occur singly and are therefore open for 100% of the time. Thus no clear prediction can be made about the direction of the change in the 'burst P_{open} ' that is expected if the channel opening rate, β , is reduced. This happens essentially because a burst must have a number of openings that is always 1 more than the number of shuttings. In order to make a definition of 'burst P_{open} ' that is based on equal numbers of open and shut times, one (arbitrary) procedure is to subtract one mean open time from the numerator (mean open time per burst) and from the denominator (mean burst length). This calculation was done using the mean open period (which is likely to provide an over-correction since it is extended by missed shuttings). The modified 'burst P_{open} ' is also found to be increased by the mutation (from 0.32 ± 0.05 in wild-type receptors, to 0.87 ± 0.02 in mutant receptors). The interesting thing about this modified 'burst P_{open} ' is that it is expected to increase monotonically with both β and k_{-2} . For Scheme 1 it is given by:

$$\frac{1}{1 + \frac{\alpha}{\beta + 2k_{-2}} \left(1 + \frac{k_{+D}}{k_{-D}}\right)}$$

Thus, unlike the other observations, it distinguishes between a decrease in the opening rate, β , and an increase in the dissociation rate, k_{-2} . The former should reduce the modified 'burst P_{open} ', contrary to observation, but the latter should increase it, as observed. Additionally, the time constant of the first component present in the shut time distribution of NR1a/NR2A(T671A) NMDA receptor-channels is briefer than that seen in wild-type distributions ($21 \pm 1 \mu\text{s}$ compared with $45 \pm 8 \mu\text{s}$). This too would be expected with a mutation that increases the dissociation rate of glutamate if this component describes a short-lived shut state of the channel from which agonist can dissociate.

Comparison of current relaxations following concentration jumps with burst lengths

The present study shows that there is good agreement between the time constants that describe the decay of macroscopic currents following concentration jumps and those that describe single-channel burst lengths recorded in the steady-state (though, as usual, macroscopic measurements are not precise enough to allow all of the time constants to be estimated from observations). Such a result is to be expected if the method of isolating separate bursts in our steady-state records is adequate and if the duration of such bursts is independent of the agonist concentration (Wyllie *et al.* 1998). Table 1 shows that a 10-fold increase in the glutamate concentration does not affect burst length, suggesting that

the rate constants governing transitions within, and the exit from, burst states (set E, Colquhoun & Hawkes, 1982) are independent of concentration (in the range we have used in our steady-state recordings).

The nature of the binding site

The amino acid T671 is in the S2 domain of the NMDA receptor, which follows the third membrane domain, and which is thought to constitute one lobe of the agonist binding site, the other being formed by the S1 domain which precedes the first membrane region (reviewed by Dingledine *et al.* 1999; for alternative naming of membrane regions see Chen *et al.* 1999). Analogous regions exist in all glutamate receptors, and in the structure of a protein made by joining S1 and S2 domains of the GluR2 receptor with a short linker which has been determined by Armstrong *et al.* (1998). Alignment of the sequences of GluR2 and NR2A subunits shows that T671A in the latter is analogous with T655 in GluR2. The hydroxyl group of T655 was found by Armstrong *et al.* to form a hydrogen bond with a carboxyl group of a bound kainate molecule. Furthermore Paas *et al.* (1996) found that the analogous mutation in a chick kainate-binding protein (T268A) abolished detectable binding of kainate (though of course reduction of macroscopic binding does not constitute evidence for a change in the binding site; Colquhoun, 1998). The structure of the NMDA receptor has not been determined, but theoretical molecular modelling studies of the NR2C subunit by Chohan *et al.* (2000) give particular importance to T671 in determination of agonist binding specificity (T671 in NR2A corresponds to T691 in their paper). This residue is proposed to form a hydrogen bond with glutamate, when it occupies its binding site. Therefore it is perhaps not surprising that removing this sort of bonding between ligand and receptor has dramatic effects on glutamate potency.

Conclusion

As mentioned above a realistic kinetic scheme that describes NMDA receptor activation is a goal yet to be realised and therefore we are not in a position to determine the precise nature of the T671A mutation. However, the evidence presented here, together with that reported in our previous study (Anson *et al.* 1998), suggests strongly that the most prominent effect, by far, of the T671A mutation is to increase the rate of dissociation of glutamate from its binding site on the shut channel.

ANSON, L. C., CHEN, P. E., WYLLIE, D. J. A., COLQUHOUN, D. & SCHOEPFER, R. (1998). Identification of amino acid residues of the NR2A subunit which control glutamate potency in recombinant NR1/NR2A NMDA receptors. *Journal of Neuroscience* **18**, 581–589.

ANSON, L. C., SCHOEPFER, R., COLQUHOUN, D. & WYLLIE, D. J. A. (1999). Single-channel current properties of NMDA receptor-channels, expressed in *Xenopus* oocytes, that contain a mutation in the glutamate binding site. *Journal of Physiology* **521**, P, 90P.

- ARMSTRONG, N., SUN, Y., CHEN, G.-Q. & GOUAUX, E. (1998). Structure of a glutamate-receptor ligand-binding core in complex with kainate. *Nature* **395**, 913–917.
- BÉHÉ, P., COLQUHOUN, D. & WYLLIE, D. J. A. (1999). Activation of single AMPA- and NMDA-type glutamate-receptors channels. In *Handbook of Experimental Pharmacology*, ed. JONAS, P. & MONYER, H., vol. 141, pp. 175–218. Springer Verlag, Berlin.
- BÉHÉ, P., STERN, P., WYLLIE, D. J. A., NASSAR, M., SCHOEPFER, R. & COLQUHOUN, D. (1995). Determination of the NMDA NR1 subunit copy number in recombinant NMDA receptors. *Proceedings of the Royal Society B* **262**, 205–213.
- BLATZ, A. L. & MAGELBY, K. L. (1986). Correcting single channel data for missed events. *Biophysical Journal* **49**, 967–980.
- CHEN, G. Q., CUI, C., MAYER, M. L. & GOUAUX, E. (1999). Functional characterization of a potassium-selective prokaryotic glutamate receptor. *Nature* **402**, 817–821.
- CHOHAN, K. K., WO, Z. G., OSWALD, R. E. & SUTCLIFFE, M. J. (2000). Structural insights into NMDA ionotropic glutamate receptors via molecular modelling. *Journal of Molecular Modelling* **6**, 16–25.
- CLAPHAM, D. E. & NEHER, E. (1984). Substance P reduces acetylcholine-induced currents in isolated bovine chromaffin cells. *Journal of Physiology* **347**, 255–277.
- CLEMENTS, J. D. & WESTBROOK, G. L. (1991). Activation kinetics reveal the number of glutamate and glycine binding sites on the N-methyl-D-aspartate receptor. *Neuron* **7**, 605–613.
- COLQUHOUN, D. (1998). Binding, gating, affinity and efficacy. The interpretation of structure-activity relationships for agonists and of the effects of mutating receptors. *British Journal of Pharmacology* **125**, 923–948.
- COLQUHOUN, D. & HAWKES, A. G. (1982). On the stochastic properties of bursts of single ion channel openings and of clusters of bursts. *Philosophical Transactions of the Royal Society B* **300**, 1–59.
- COLQUHOUN, D. & SAKMANN, B. (1985). Fast events in single-channel currents activated by acetylcholine and its analogues at the frog muscle end-plate. *Journal of Physiology* **369**, 501–557.
- COLQUHOUN, D. & SIGWORTH, F. J. (1995). Fitting and statistical analysis of single-channel records. In *Single Channel Recording*, ed. SAKMANN, B. & NEHER, E., 2nd edn, pp. 483–587. Plenum Press, New York.
- CULL-CANDY, S. G., FARRANT, M. & FELDMEYER, D. (1995). NMDA channel conductance: a user's guide. In *Excitatory Amino Acids and Synaptic Transmission*, ed. WHEAL, H. V., pp. 121–132. Academic Press Limited, London.
- DINGLELINE, R., BORGES, K., BOWIE, D. & TRAYNELIS, S. F. (1999). The glutamate receptor ion channels. *Pharmacological Reviews* **51**, 7–61.
- GIBB, A. J. & COLQUHOUN, D. (1992). Activation of N-methyl-D-aspartate receptors by L-glutamate in cells dissociated from adult rat hippocampus. *Journal of Physiology* **456**, 143–179.
- HIRAI, H., KIRSCH, J., LAUBE, B., BETZ, H. & KUHSE, J. (1996). The glycine binding site of the N-methyl-D-aspartate receptor subunit NR1: Identification of novel determinants of co-agonist potentiation in the extracellular M3-M4 loop region. *Proceedings of the National Academy of Sciences of the USA* **93**, 6031–6036.
- KURYATOV, A., LAUBE, B., BETZ, H. & KUHSE, J. (1994). Mutational analysis of the glycine-binding site of the NMDA receptor: Structural similarity with bacterial amino acid-binding proteins. *Neuron* **12**, 1291–1300.
- LAUBE, B., HIRAI, H., STURGESS, M., BETZ, H. & KUHSE, J. (1997). Molecular determinants of agonist discrimination by NMDA receptor subunits: Analysis of the glutamate binding site on the NR2B subunit. *Neuron* **18**, 493–503.
- LESTER, R. A. J. & JAHR, C. E. (1992). NMDA channel behavior depends on agonist affinity. *Journal of Neuroscience* **12**, 635–643.
- LUMMIS, S. C. R., FLETCHER, E. J. & GREEN, T. (1998). NMDA receptor NR2 subunits contain amino acids involved in glutamate binding. *Journal of Physiology* **506.P**, 76P.
- MAGLEBY, K. L. & PALLOTTA, B. S. (1983). Burst kinetics of single calcium-activated potassium channels in cultured rat muscle. *Journal of Physiology* **344**, 605–623.
- PAAS, Y., EISENSTEIN, M., MEDEVIELLE, F., TEICHBERG, V. I. & DEVILLERS-THIERY, A. (1996). Identification of the amino acid subsets accounting for the ligand binding specificity of a glutamate receptor. *Neuron* **17**, 979–990.
- SIGWORTH, F. J. & SINE, S. M. (1987). Data transformations for improved display and fitting of single-channel dwell time histograms. *Biophysical Journal* **52**, 1047–1054.
- SINE, S. M., OHNO, K., BOUZAT, C., AUERBACH, A., MILONE, M., PRUITT, J. N. & ENGEL, A. G. (1995). Mutation of the acetylcholine receptor α subunit causes a slow-channel myasthenic syndrome by enhancing agonist binding affinity. *Neuron* **15**, 229–239.
- SIVILOTTI, L. G., MCNEIL, D. K., LEWIS, T. M., NASSAR, M. A., SCHOEPFER, R. & COLQUHOUN, D. (1997). Recombinant nicotinic receptors, expressed in *Xenopus* oocytes, do not resemble native rat sympathetic ganglion receptors in single-channel behaviour. *Journal of Physiology* **500**, 123–138.
- STERN, P., BÉHÉ, P., SCHOEPFER, R. & COLQUHOUN, D. (1992). Single channel conductances of NMDA receptors expressed from cloned cDNAs: comparison with native receptors. *Proceedings of the Royal Society B* **250**, 271–277.
- WAFFORD, K. A., KATHORIA, M., BAIN, C. J., MARSHALL, G., LE BOURDELLES, B., KEMP, J. A. & WHITING, P. J. (1995). Identification of amino acids in the N-methyl-D-aspartate receptor NR1 subunit that contribute to the glycine binding site. *Molecular Pharmacology* **47**, 374–380.
- WILLIAMS, K., CHAO, J., KASHIWAGI, K., MASUKO, T. & IGARASHI, K. (1996). Activation of N-methyl-D-aspartate receptors by glycine: Role of an aspartate residue in the M3-M4 loop of the NR1 subunit. *Molecular Pharmacology* **30**, 701–708.
- WYLLIE, D. J. A., BÉHÉ, P. & COLQUHOUN, D. (1998). Single-channel activations and concentration jumps: comparison of recombinant NR1a/NR2A and NR1a/NR2D NMDA receptors. *Journal of Physiology* **510**, 1–18.
- WYLLIE, D. J. A., BÉHÉ, P., NASSAR, M., SCHOEPFER, R. & COLQUHOUN, D. (1996). Single-channel currents from recombinant NMDA NR1a/NR2D receptors expressed in *Xenopus* oocytes. *Proceedings of the Royal Society B* **263**, 1079–1086.

Acknowledgements

We are grateful to Professor A. G. Hawkes for his comments on the display of geometric distributions. R.S. is a Wellcome Trust Senior Research Fellow. D.J.A.W. held a Royal Society University Research fellowship in the Department of Pharmacology, University College London for the duration of this work. This work was supported by the Wellcome Trust, MRC and the Royal Society.

Corresponding author's present address

D. J. A. Wyllie: Department of Neuroscience, University of Edinburgh, 1 George Square, Edinburgh EH8 9JZ, UK.

Email: david.j.a.wyllie@ed.ac.uk

Author's present address

L. C. Anson: Nature Editorial Office, Macmillan Magazines Ltd, Porters South, 4–6 Crinan Street, London N1 9XW, UK.